Dephasing of a superconducting flux qubit

K. Kakuyanagi[1], T. Meno[2], S. Saito[1], H. Nakano[1], K. Semba[1], H. Takayanagi[3], F. Deppe[4], and A. Shnirman[5]

[1]*NTT Basic Research Laboratories, NTT Corporation, Kanagawa, 243-0198, Japan*
[2]*NTT Advanced Technology, NTT Corporation, Kanagawa, 243-0198, Japan*
[3]*Tokyo University of Science, 1-3 Kagurazaka, Shinjuku, Tokyo 162-8601, Japan*
[4]*Walther-Meißner-Institut,Walther-Meißner-Str. 8, D-85748 Garching, Germany*
[5]*Institut für Theoretische Festkörperphysik, Universität Karlsruhe, D-76128 Karlsruhe, Germany*

In order to gain a better understanding of the origin of decoherence in superconducting flux qubits, we have measured the magnetic field dependence of the characteristic energy relaxation time (T_1) and echo phase relaxation time (T_2^{echo}) near the optimal operating point of a flux qubit. We have measured T_2^{echo} by means of the phase cycling method. At the optimal point, we found the relation $T_2^{\text{echo}} \approx 2T_1$. This means that the echo decay time is *limited by the energy relaxation* (T_1 process). Moving away from the optimal point, we observe a *linear* increase of the phase relaxation rate ($1/T_2^{\text{echo}}$) with the applied external magnetic flux. This behavior can be well explained by the influence of magnetic flux noise with a $1/f$ spectrum on the qubit.

As a consequence of the progress in the microfabrication technology, in the last years solid-state based artificial quantum two level systems (TLS), which can be fabricated, operated and read out in a controlled way have been successfully realized [1, 2]. These artificial TLS can be used as quantum bits (qubits), i.e. the fundamental devices for quantum information systems [3].

Among the solid state based qubits one of the most promising candidates are the Josephson junction based qubits [1, 2, 4]. Because superconductivity is a macroscopic quantum phenomenon, superconducting qubits have an inherent advantage over qubits based on microscopic systems such as single atoms [5]. Furthermore, Josephson junction based qubits also represent promising candidates for the study of fundamental aspects of macroscopic quantum systems [6]. For these studies , long coherence time as well as high readout fidelity are required. Evidently, the fidelity can be improved by refining the detection method, such as Josephson bifurcation amplifier technique [7]. However, decoherence is still determined by the environment of the qubit. Thus, in order to reduce decoherence we have to first understand its origin in detail.

In this letter, we present a systematic study of the dephasing in a superconducting flux qubit whose level splitting is sensitive to the applied external magnetic flux. This allows us to investigate the dependence of the coherence time on the applied flux bias. It is expected that such a measurement gives information on the interdependence between the qubit decoherence and the magnetic fluctuations. We present experimental results on the magnetic flux dependence of both the energy relaxation time (T_1) and the echo phase decay time (T_2^{echo}) of a superconducting flux qubit. Based on our data, we discuss possible mechanisms responsible for decoherence in superconducting flux qubits. As a result, we find that at the optimal point the coherence time is limited by the energy relaxation (T_1 process). Away from the optimal point, the phase relaxation time is determined by $1/f$
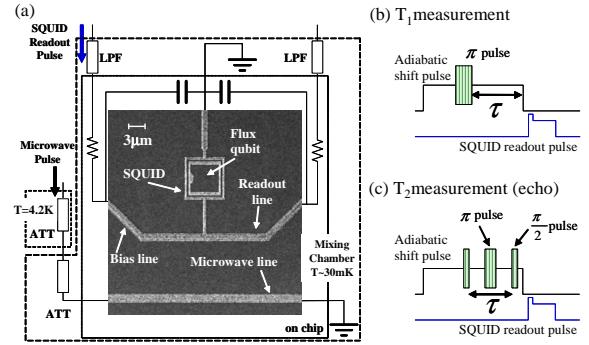

FIG. 1: (color online). (a) Scanning electron micrograph of the sample . Three Josephson junction flux qubit is surrounded with a SQUID detector loop. We apply MW and adiabatic dc shift pulse via the MW-line. The mutual inductance between the MW-line and the flux qubit is ~ 1 pH. The readout pulse is applied via the current bias line and qubit state is detected by measuring the voltage through the readout line. We use copper powder filter as low-pass filter (LPF) of these lines. (b) Pulse sequence for the T_1 measurement. We generate composite pulse by adding adiabatic DC pulse and MW pulse. The dc-SQUID readout pulse is programmed to reach the sample just after the adiabatic shift pulse is turned off. A rising time of each MW pulse is faster than 0.5 ns. The π pulse width is about ~ 2 ns. (c) Pulse sequence for the T_2^{echo} measurement. In order to avoid a reduction of the visibility by the T_1 process, we programmed the end of the adiabatic shift pulse and the start of the readout pulse to be reached to the sample as soon as the second $\pi/2$ pulse finished.

magnetic fluctuations.

The sample consists of a three junction flux qubit which is surrounded by a dc SQUID [8]. Unlike in other qubit designs [2], the SQUID loop does not share a current line with the qubit loop. Thus the coupling between qubit and readout SQUID is purely inductive (see Fig. 1(a)) with the mutual inductance ~ 13 pH. The electromagnetic environment of the qubit is engineered by

equipping the SQUID detector with an on-chip shunting capacitor. For the fabrication of the Al-Al_2O_3-Al Josephson junctions we used usual angled shadow evaporation technique [9]. The sample was mounted in a dilution refrigerator and cooled it down below 50mK.

At the optimal flux bias point, the mean value of the persistent current vanishes for both states of the qubit. To be able to discriminate between the two states of the qubit at this operation point, we used the adiabatic shift pulse method as illustrated in Fig. 1(b,c) [10]. Then we apply an adiabatic magnetic dc-pulse with a rise time of 0.8 ns to the qubit through the coplanar RF-line. The qubit operation is performed during this adiabatic shift pulse. At the end of the shift pulse, the qubit will move back to the initial bias point adiabatically, where the readout can be done. In this way we can get information about the qubit state even close to the optimal point.

We first performed MW spectroscopy of the qubit. The resonant frequency (corresponding to the energy splitting of the qubit) is determined by saturating the state of the qubit with a long enough MW pulse and measuring the SQUID switching probability afterwards. Figure. 2 shows the result obtained for the magnetic flux dependence of the level splitting of the qubit. In the two-level approximation the qubit Hamiltonian is $H_{qb} = \frac{1}{2} \left(\epsilon(\Phi_x)\sigma_z + \Delta\sigma_x \right)$, where $\epsilon(\Phi_x)$ is the level splitting induced by the external flux Φ_x threading the qubit loop and σ_x, σ_z are the Pauli matrices. From the spectroscopy experiment we determined the qubit gap frequency (i.e. the energy splitting at the optimal point) to be $\Delta/h = 3.9$ GHz, where h is the Planck constant. We also found the persistent current away from the optimal point, $\frac{h}{2}\frac{\partial\epsilon}{\partial\Phi_x} = I_p = 370$ nA.

Next, we measured the magnetic flux dependence of T_1 and T_2^{echo}. T_1 is the energy relaxation time describing the transition of the qubit from the excited state to the ground state due to the interaction with the environment
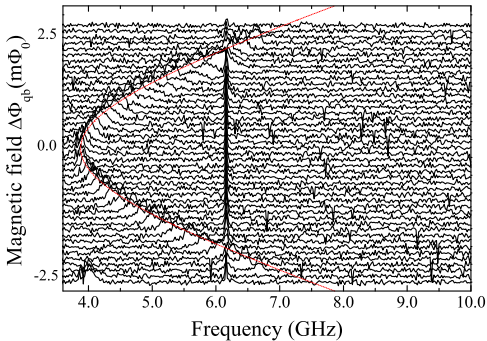

FIG. 2: (color online). Magnetic flux dependence of frequency sweep spectrum. The qubit spectrum is observed as a hyperbola. The field insensitive resonance at 6.2 GHz is attributed to the on-chip LC resonator [10]. The red dotted line represents a fit of the qubit spectrum by a hyperbolic function.
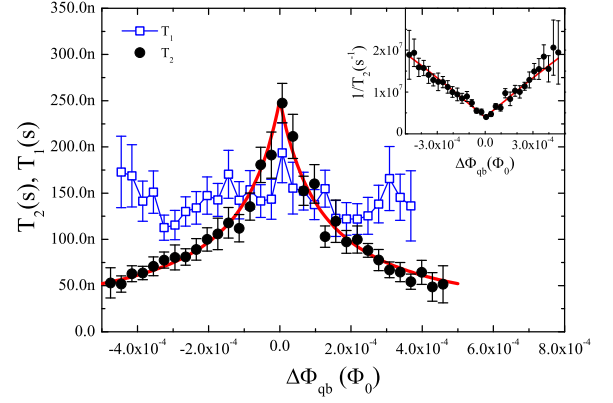

FIG. 3: (color online). Magnetic flux dependence of T_1 (open squares) and T_2^{echo} (filled circles). Although there is considerable scatter in the T_1 data, obviously there is only a weak flux dependence. The largest T_2^{echo} values are obtained at the optimal point. Since the T_2^{echo} data have been obtained via the phase cycling technique, the difference of the magnitude of error bars of T_1 and T_2^{echo} is due to differences in the averaging number (each T_2^{echo} value is obtained from roughly eight times as many data as the T_1 value) [13].

(for $k_BT \ll \Delta$). In order to measure T_1, we use the pulse sequence shown in Fig. 1(b). Repeating this sequence provides the relaxation probability as a function of the waiting time. T_1 is obtained by an exponential fit of this curve. The T_2^{echo} time is the decay time in the echo experiments depicted in Fig. 1(c).

To understand the effect of non-ideal control in the echo sequence we calculate the state of the qubit after applied three pulse sequence in the absence of fluctuations. The integrals (rotation angles) of the three pulses are θ_1, θ_2 and θ_3. The time interval between the first and the second pulses is τ_1, while between the second and the third pulse it is τ_2. We assume that the initial qubit state is along the z-axis of the Bloch sphere and calculate the z-axis projection of the final state $\langle\sigma_z\rangle$:

$$
\begin{aligned}
\langle\sigma_z\rangle = \ & \cos\theta_1\cos\theta_2\cos\theta_3 - \sin\theta_1\sin\theta_2\cos\theta_3\cos\delta\omega\tau_1 \\
& - \cos\theta_1\sin\theta_2\cos\theta_3\cos\delta\omega\tau_2 \\
& - \sin\theta_1\left(\cos\theta_2+1\right)\sin\theta_3\cos\left(\delta\omega\left(\tau_1+\tau_2\right)\right)/2 \\
& - \sin\theta_1\left(\cos\theta_2-1\right)\sin\theta_3\cos\left(\delta\omega\left(\tau_1-\tau_2\right)\right)/2 \quad (1)
\end{aligned}
$$

Here, $\delta\omega$ is the detuning. For an ideal echo sequence we have $\theta_1 = \theta_3 = \pi/2$, $\theta_2 = \pi$, and $\tau_1 = \tau_2$. Under these conditions only the fifth term of Eq. (1), the so-called echo term, survives and it is independent of $\tau = \tau_1 + \tau_2, (\tau_1 = \tau_2)$ [11]. By using phase modulated pulses we can control the rotation axis of the Bloch vector [12] for all three pulses of the echo sequence [13]. The phase cycling method makes it possible to extract only the echo term. We are able to obtain stable echo decay curve during long time experiment.

Figure. 3 shows the magnetic flux dependence of T_1 and T_2^{echo} in the vicinity of the optimal point. The T_1 values show some scatter but the flux dependence of T_1 is weak. On the other hand, the T_2^{echo} values show a pronounced flux dependence. In particular, there is a sharp maximum at the optimal point. This tendency was also reported for the edge shared SQUID-flux qubit by Bertet et al. [14]. At the optimal point, we have $T_2^{\text{echo}} > T_1$.

It is well known [15] that the energy relaxation contributes to the dephasing process via

$$\left(T_2^{\text{echo}}\right)^{-1} = (2T_1)^{-1} + \Gamma_\varphi \ . \tag{2}$$

Here Γ_φ is the pure dephasing rate due to the fluctuations in the energy splitting of the qubit. The dephasing rate Γ_φ consists of two contributions $\Gamma_\varphi = \Gamma_\varphi^0 + \Gamma_\varphi^\Phi$. Γ_φ^0 should be identified with the non-magnetic dephasing processes or with the second-order contribution [16]. Γ_φ^Φ is the first-order contribution due to magnetic dephasing processes. At the optimal point, the magnetic flux derivative of the energy dispersion is flat $\left|\frac{\partial \Delta E}{\partial \Phi}\right| = 0$, and there is no contribution of first-order magnetic flux fluctuations to the dephasing rate, i.e. $\Gamma_\varphi^\Phi = 0$. We obtain $T_2^{\text{echo}} = 250$ ns at the optimal point and the average value of T_1 around the optimal point is about 140 ns. From these values, we estimate the pure dephasing rate at the optimal point to be $\Gamma_\varphi^0 = (2.3 \mu s)^{-1}$. *Remarkably, the dephasing time of the qubit* (T_2^{echo}) *is almost entirely determined by the energy relaxation process, i.e.* $T_2^{\text{echo}} \approx 2T_1$. In other words, the dephasing of the flux qubit near the optimal point is predominantly determined by the high-frequency noise $S_\Phi(\omega \approx \Delta/\hbar)$.

For dephasing dominated by magnetic flux noise with a smooth spectrum near $\omega = 0$ this rate is given by

$$\Gamma_\varphi^\Phi = \frac{1}{2} \left|\frac{\partial \Delta E}{\partial \Phi_x}\right|^2 S_\Phi(\omega = 0) \ . \tag{3}$$

Here $\Delta E \equiv \Delta E(\Phi_x)$ is the external, flux dependent qubit energy splitting and $S_\Phi(\omega = 0)$ is the low frequency component of a correlation function of flux fluctuations. From $\Delta E = \sqrt{\epsilon^2(\Phi_x) + \Delta^2}$ we obtain $\partial \Delta E/\partial \Phi_x = \cos \eta \,(\partial \epsilon/\partial \Phi_x)$, where $\tan \eta = \Delta/\epsilon$. Since the variation of the bias with external flux, $\partial \epsilon/\partial \Phi_x$, is usually almost constant over a wide interval of the applied flux. Γ_φ^Φ becomes proportional to $\cos^2 \eta$. Taking into account that, according to our experimental findings, the T_1 time is almost independent of the applied flux and that a relation $\cos \eta \propto \epsilon$ is satisfied near the optimal point, a parabolic behavior of $1/T_2^{\text{echo}}$ is expected in this region. However, as shown in the inset of Fig. 3 the measured $1/T_2^{\text{echo}}$ versus applied flux curve is linear. This result is very different from the prediction of Eq. (3). As a consequence, our experimental data cannot be explained with a simple Bloch-Redfield type of decoherence theory where a noise with short correlation time (white noise near $\omega = 0$) is assumed. In order to explain the observed behavior we need to consider decoherence from a long correlated noise.

Even when the pure dephasing is non-exponential the echo decay curve can be represented as the product of energy decay (T_1) and pure phase decay. In this case Eq. (2) is replaced by a non-exponential decay curve for the expectation value of σ_z at the end of the echo sequence $\rho(t) \equiv \langle \sigma_z \rangle = \exp\left(-\frac{t}{2T_1}\right) \cdot \rho_{\text{echo}}(t)$, where $\rho_{\text{echo}}(t) = \left\langle \exp\left\{-i \left(\frac{\partial \epsilon}{\partial \Phi}\right) \cos \eta \left[\int_0^{\frac{t}{2}} \Phi(\tau)\, d\tau - \int_{\frac{t}{2}}^t \Phi(\tau)\, d\tau\right]\right\}\right\rangle$. Assuming Gaussian flux fluctuations this gives $\rho_{\text{echo}}(t) = \exp\left[-\frac{1}{2}\left(\frac{\partial \epsilon}{\partial \Phi}\right)^2 \cos^2 \eta \int \frac{d\omega}{2\pi} S_\Phi(\omega) \frac{\sin^4 \frac{\omega t}{4}}{\left(\frac{\omega}{4}\right)^2}\right]$. In the case of white noise, $S_\Phi(\omega) = \text{const.}$, $\rho_{\text{echo}}(t)$ gives a simple exponential decay curve, and the flux dependence of the decay rate follows Eq. (3). On the other hand, for $S_\Phi(\omega) = \frac{A}{f} = \frac{2\pi A}{\omega}$ ($1/f$-noise [17]) $\rho_{\text{echo}}(t) = \exp\left[-t^2 \cdot \left(\frac{\partial \epsilon}{\partial \Phi}\right)^2 \cdot \cos^2 \eta \cdot A \cdot \ln 2\right]$. This decay law is Gaussian and the relaxation rate is proportional to $\left|\frac{\partial \epsilon}{\partial \Phi} \cos \eta\right|$.

We do not attempt to determine the echo decay shape from the observed relaxation curve because our experimental data do not have precision enough to distinguish between the different types of decay curves (e.g. simple exponential, Gaussian or algebraic). Instead, we assume a special decay shape based on the $1/f$ fluctuations spectrum $\rho(t) = \exp\left(-\frac{t}{2T_1}\right) \cdot \exp\left(-\Gamma_\varphi^0 t\right) \cdot \exp\left(-\Gamma_\varphi^{\Phi 2} t^2\right)$. And we find the magnetic flux dependence of Γ_φ^Φ by fitting of this formula. In this fitting T_1 and Γ_φ^0 are fixed and Γ_φ^Φ is the fitting parameter. This relaxation function is constructed from three components. The first one describes the energy relaxation (T_1 process). In the second component Γ_φ^0 is the phase relaxation rate, which
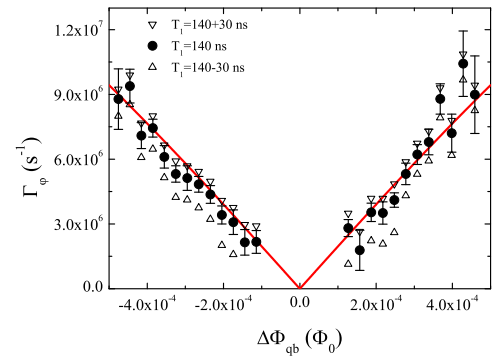

FIG. 4: (color online). Magnetic flux dependence of Γ_φ values. The Γ_φ values are derived from fits of the data by the $1/f$ fluctuation model using a constant T_1 value. The filled circles represent Γ_φ values estimated using an average T_1 value of 140 ns. Since the T_1 values have some scattering, we also estimated Γ_φ values using both $T_1 = 140 \pm 30$ ns. The triangles and inverted triangles represent the Γ_φ values estimated from $T_1 = 110$ ns and 170 ns, respectively. The red solid line shows a linear fit to the Γ_φ data.

is caused by non-magnetic fluctuations [18] and second-order contributions of magnetic fluctuations. Near the optimal point, the second-order Φ_x contributions of Γ_φ^0 is small then we can neglect it. Finally, Γ_φ^Φ is the phase relaxation rate due to $1/f$ magnetic fluctuations. We obtain $T_1 = 140$ ns from the energy relaxation curve and $\Gamma_\varphi^0 = (2.3\ \mu\mathrm{s})^{-1}$ from the echo decay rate at the optimal point. Figure. 4 shows the magnetic flux dependence of the resulting Γ_φ^Φ. Very close to the optimal point, the contribution of Γ_φ^Φ to the echo decay curve is very small compared to that of $1/T_1$. In this region the Γ_φ^Φ values cannot be extracted with sufficient accuracy from the echo decay curve. Apart from this region, the magnetic flux dependence of Γ_φ^Φ is well fitted by expression $\Gamma_\varphi^\Phi \propto \left|\frac{\partial \Delta E}{\partial \Phi}\right| = \left|\frac{\partial \epsilon}{\partial \Phi}\cos\eta\right|$. This means that Γ_φ^Φ is proportional to absolute value of the magnetic flux difference from the optimal point. Thus our experimental result suggests the existence of $1/f$ type magnetic fluctuations in the frequency range of $\omega \approx O\left(\Gamma_\varphi^\Phi\right)$. The magnitude of the $1/f$ flux noise can be estimated for the A value of the correlation function $S_\Phi\left(\omega\right) = \frac{2\pi A}{\omega}$. From the spectrum dispersion and the magnetic flux dependence of Γ_φ^Φ we obtain $A \approx \left(10^{-6}\Phi_0\right)^2$. This value is of the same order as for other superconducting circuit [19].

In summary, we have performed a systematic study of the phase and energy relaxation of a superconducting flux qubit by measuring the magnetic flux dependence of the energy relaxation (T_1) time and of the echo decay time (T_2^{echo}). At the optimal point we find that the contribution of magnetic fluctuations is negligible. The T_2^{echo} time of the qubit is then determined by the energy relaxation resulting in $T_2^{\mathrm{echo}} \approx 2T_1$. Thus, in order to improve the coherence time of our flux qubit at the optimal point, *we need to suppress high frequency transversal fluctuations $S_{x,y}\left(\Delta/\hbar\right)$*. Away from the optimal point the magnetic flux fluctuations dominate the echo dephasing time T_2^{echo}. The observed linear dependence of Γ_φ^Φ on magnetic flux around the optimal point suggests that *the magnetic fluctuations have a $1/f$-type spectrum in a frequency range of the order of $1/T_2^{\mathrm{echo}}$*. To our knowledge these results provide the first experimental clue for the possible origin of decoherence in a superconducting flux qubit, which is not sharing an edge with its dc SQUID detector.

Note added: After complete this work, we became aware of similar results by F. Yoshihara *et al.* [20].

[1] Y. Nakamura, Yu. A. Pashkin, J. S. Tsai, Nature **389**, 786 (1999) , D. Vion, A. Aassime, A. Cottet, P. Joyez, H. Pothier, C. Urbina, D. Esteve, M. H. Devoret, Science **296**, 886 (2002) , J. M. Martinis, S. Nam, J. Aumentado, Phys. Rev. Lett. **89** 117901 (2002)

[2] I. Chiorescu, Y. Nakamura, C. J. P. M. Harmans, J. E. Mooij, Science **299**, 1869 (2003)

[3] A. Barenco, D. Deutsch, A. Ekert, R. Joza, Phys. Rev. Lett.**74** 4083 (1995)

[4] J. E. Mooij, T. P. Orlando, L. Levitov, L. Tian, C. H. van der Wal, S. Lloyd, Science **285**, 1036 (1999)

[5] Y. Makhlin, G. Schön, A. Shnirman, Rev. Mod. Phys. **73**, 357 (2001). , F. K. Wilhelm and K. Semba, *Physical Realizations of Quantum Computing*, World Scientific, 2006. p.38-107

[6] A. J. Leggett, A. Garg, Phys. Rev. Lett.**54** 857 (1985) , C. D. Tesche, Phys. Rev. Lett.**64** 2358 (1990)

[7] I. Siddiqi, R. Vijay, M. Metcalfe, E. Boaknin, L. Frunzio, R. J. Schoelkopf, and M. H. Devoret, Phys. Rev. B.**73** 054510 (2006)

[8] S. Saito *et al.* , Phys. Rev. Lett. **93**, 037001 (2004)

[9] S. Saito *et al.* , Phys. Rev. Lett. **96**, 107001 (2006)

[10] J. Johansson, S. Saito, T. Meno, H. Nakano, M. Ueda, K. Semba, H. Takayanagi, Phys. Rev. Lett. **96**, 127006 (2006)

[11] If the echo conditions are satisfied only approximately, e.g. because of non-perfect $\pi/2$ or π pulses, other terms may contribute. The fact that these terms depend on $\delta\omega\tau$ explains some of the beatings in the echo decay curve observed sometimes in our experiments.

[12] E. Collin, G. Ithier, A. Aassime, P. Joyez, D. Vion, D. Esteve, Phys. Rev. Lett. **93**, 157005 (2004) ,T. Kutsuzawa *et al.* , Appl. Phys. Lett.**87**,073501 (2005)

[13] We have four choices of the second pulse phase ($0°$, $90°$, $180°$, $270°$) and two for the first pulse phase ($0°$, $180°$) as a pulse sequence. There are eight combinations of these pulse phases. By the sign of the fifth term of Eq. (1), we add or subtract echo decay data of each pulse combination.

[14] P. Bertet, I. Chiorescu, G. Burkard, K. Semba, C. J. P. M. Harmans, D. P. DiVincenzo, J. E. Mooji, Phys. Rev. Lett. **95**, 257002 (2005)

[15] R. K. Wangsness and F. Bloch, Phys. Rev. **89**, 728 (1953) , A. G. Redfield, IBM J. Res. Dev. **19**, 1 (1957)

[16] Y. Makhlin and A. Shnirman, Phys. Rev. Lett. **92**, 178301 (2004)

[17] O. Astafiev, Y. A. Pashkin, Y. Nakamura, T. Yamamoto, J. S. Tsai, Phys. Rev. Lett. **96**, 137001 (2006) , J. Schriefl, Y. Makhlin, A. Shnirman, G. Schön , New J. Phys. **8**, 1 (2006)

[18] Γ_φ^0 may be caused by SQUID bias current fluctuations. But contributions of bias current fluctuations are weak. The coupling between our sample's qubit and SQUID is weak, because our qubit sample does not share any edges of qubit and SQUID.

[19] F. C. Wellstood, C. Urbina, J. Clarke , Appl. Phys. Lett. **50**, 772 (1987) , F. C. Wellstood, C. Urbina, J. Clarke , Appl. Phys. Lett. **85**, 5296 (2004)

[20] F. Yoshihara, K. Harrabi, A. O. Niskanen, Y. Nakamura, J. S. Tsai, cond-mat/0606481